

# RADIOACTIVITY CONCENTRATIONS AND DOSE CHARACTERISTICS OF GRANITE STONES

by

**Rahim KHABAZ**<sup>1\*</sup> and **Maryam HASSANVAND**<sup>2</sup>

<sup>1</sup> Physics Department, Faculty of Sciences, Golestan University, Gorgan, Iran

<sup>2</sup> Department of Physics, Isfahan University of Technology, Isfahan, Iran

Scientific paper

<http://doi.org/10.2298/NTRP1703275K>

We obtained the radionuclide concentrations of <sup>238</sup>U, <sup>232</sup>Th, and <sup>40</sup>K in various samples of the granite stones by measuring with a high efficiency NaI(Tl) (10.16 cm × 10.16 cm) scintillation detector. The activities of <sup>238</sup>U, <sup>232</sup>Th, and <sup>40</sup>K were recorded and determined by a full-spectrum analysis. The concentrations of radionuclides were found to be in ranges of 32.3-92.6 Bqkg<sup>-1</sup>, 23.9-52.2 Bqkg<sup>-1</sup>, and 796.5-2018.4 Bqkg<sup>-1</sup> for <sup>238</sup>U, <sup>232</sup>Th, and <sup>40</sup>K, respectively. The radiological dose rates and the hazard indices were also calculated in this analysis.

*Key words:*  $\gamma$ -ray spectrometry, NaI(Tl), radioactivity, dose characteristic, granite, MCNPX

## INTRODUCTION

Granite is one of the most popular materials used in buildings, both for interior and exterior parts. Like the other environmental materials, granite has natural radioactivity. The radioactivity concentration varies from region to region in a country. The main contribution of radioactivity to the external exposure belongs to <sup>238</sup>U, <sup>232</sup>Th, and <sup>40</sup>K nuclei. The natural radioactivity of granite stones is generally high [1, 2]. Monitoring and measurements of the concentrations of these radionuclides in the environmental materials are substantially important to determine their activities at the time and provide adequate protections. By means of the developed techniques for measuring radioactivity levels, the accuracy of the natural radioactivity monitoring increases.

So far a number of studies have been done in a couple of countries [3-6]. In ref. [3], the authors investigated the activity concentrations and dose rates of the decorative granite in U.S. In refs. [4, 7, 8], the authors evaluated the activity on the granite stones in Egypt. Several studies also referred to the measurements of radioactivity concentrations in the soil and rocks of the local regions [9, 10]. In Iran, a few studies have also been done especially in Ramsar, a city in Northern Iran [11]. Another study [12] evaluated radon exhalation rate from granite stones. Asgharizadeh *et al.* [13], measured radioactivity concentrations of <sup>226</sup>Ra, <sup>232</sup>Th, and <sup>40</sup>K in the limited number of

granite stones in Tehran, the capital of Iran. A key limitation of these studies is that the activities of <sup>232</sup>Th and <sup>226</sup>Ra have only been determined by taking the mean activity of photo peaks of some daughter nuclides. Furthermore, the activity levels of radionuclides in the samples have been achieved by comparing methods using reference materials.

The main concern of the present work is to evaluate the natural radioactivity of the decorative granite in Iran market. In this study, using a relatively large NaI(Tl) scintillation detector having a high efficiency, we measured the <sup>238</sup>U, <sup>232</sup>Th, and <sup>40</sup>K activity levels in 19 samples of decorative granite stones collected from some parts of Iran. Then the full spectrum analysis was done [3, 14] and Monte Carlo code MCNPX was used for the detector efficiency, gamma conversion, and self-absorption corrections [15].

## MATERIALS AND METHODS

### Experimental measurements and sample preparation

Nineteen different types of decorative granite samples were collected from different cities of Iran: including Urmia (1), Zanjan (2,3), Qazvin (4), Hamedan-black (5), Borujerd (6), Isfahan (7-9), Yazd (10-12), Nehbandan (13-15), Zahedan (16-18) and Taibad (19). The samples were cut into a square shapes) 10 cm × 10 cm) with the height ranged ranging from 1.6 cm to 2.0 cm.

\* Corresponding author; e-mail: r.khabaz@gu.ac.ir  
ra\_khabaz@yahoo.com

Sodium iodide scintillator detectors activated by thallium are widely applied for gamma-rays detection because of their high efficiency and relatively acceptable energy resolution. Therefore, the granite samples were placed in front of a 10.16 cm × 10.16 cm NaI(Tl) scintillation detector coaxially with the crystal. In all cases, the distance between the samples and the detector was 2 mm.

The main measurement electronics consisted of an NaI(Tl) detector having a photomultiplier tube (PMT) which was connected to a bias supply running at 900 V, a preamplifier, and a spectroscopy amplifier. All received signals from the amplifier were digitalized by a multi-channel analyzer (MCA) and a PC.

By increasing measuring times, the accuracy of the measurement improved. Thus, gamma spectrometry was done in  $10^4$  seconds for each sample while the lower threshold energy was 0.1 MeV. During spectrometry, the system was calibrated with  $^{137}\text{Cs}$  and  $^{60}\text{Co}$  sources to set the MCA energy scale.

To prevent the detector from background and backscattered radiation, the outer cylinder of scintillation detector was covered with 4.3 cm lead shielding and all sides of the samples were surrounded by a 5 cm-thick lead blocks.

The counting rate provided by the applied detector is proportional to the radioactivity in the samples. The background spectrum was measured and subtracted from the signals. The main sources of gamma-rays from natural materials are  $^{238}\text{U}$ ,  $^{232}\text{Th}$ , and  $^{40}\text{K}$ .

### Simulation procedures

The detection of gamma ray emitted from granite stone in NaI(Tl) scintillation detector was modeled by MCNPX2.6 radiation transport code. The simulation was done to assess the response and efficiency of the detector under irradiation by granite sample. For this purpose, a cylindrical sample of granite stone with diameter of 10.16 cm and thickness of 1.8 cm was placed at a distance of 2 mm from NaI(Tl) detector. The granite density was  $2.69 \text{ gcm}^{-3}$  whose elemental composition was 48.42 % O, 2.73 % Na, 0.43 % Mg, 7.62 % Al, 33.62 % Si, 3.41 % K, 1.30 % Ca, 0.18 % Ti, 0.04 % Mn, 2.16 % Fe, and 0.10 % Pb [16]. These density and elemental composition were used for all granite samples, because they are the world-wide average density and customary elemental composition for granite. The gamma ray sources have randomly been considered within this sample, which emitted photons into 4 . Therefore, gamma conversion and self-absorption could be taken.

Three separate calculations were done for the gamma-ray spectra from the naturally occurring radioactive isotopes  $^{40}\text{K}$ ,  $^{238}\text{U}$ , and  $^{232}\text{Th}$ . For  $^{40}\text{K}$  source, the energy of gamma was 1.4608 MeV. The gamma ray en-

**Table 1. The number of gamma lines, and the average number of gammas emitted per disintegration of the parent [17]**

Parent	Number of lines	$N_{\gamma/d}$
$^{238}\text{U}$	84	2.41
$^{232}\text{Th}$	100	4.13
$^{40}\text{K}$	1	0.107

ergies and intensities for the  $^{238}\text{U}$  and  $^{232}\text{Th}$  decay series were considered based on [17]. In these energy spectra, the absolute intensities have been normalized to 100 decays of the parent nucleus assuming secular equilibrium of the uranium and thorium decay series and limited to intensities higher than or equal to 0.1 gamma rays per 100 decays of the parent nucleus. The number of gamma lines and the average number of gammas emitted per disintegration of the parent achieved by integrating the spectra are listed in tab. 1.

To determine the response of the NaI(Tl) scintillator, an F8:p tally was used to produce an energy pulse distribution created in a volume representing a physical detector. The responses were calculated in terms of the expected pulse-height spectra observed in a MCA using 256 channels. In MCNPX calculations, the energy resolution of NaI(Tl) scintillation detector was defined as 10.73 % at  $E_{\text{Ego}} = 0.662 \text{ MeV}$  (*i. e.*, the Gaussian energy broadening of MCNPX calculated pulse-height spectra was defined according to  $\text{FWHM} = a b(E cE^2)^{1/2}$  where  $a$ ,  $b$ , and  $c$  are user-supplied coefficients and  $E$  equals  $E_0$ ) [18].

## RESULTS AND DISCUSSION

### Activity concentrations

For 19 granite samples, the measurements were performed to achieve the related gamma pulse height spectra. To obtain the activity concentration for each granite sample, the related measured pulse-height spectrum was fitted to three calculated spectra achieved from Monte Carlo simulation.

The multiple linear regressions ( $\chi^2$  minimization) were performed based on Genetic algorithms using statistical computing software (R- software). The multiple linear regression is used to explain the relationship between measured pulse-height spectrum (dependent variable) from three calculated spectra of  $^{238}\text{U}$ ,  $^{232}\text{Th}$ , and  $^{40}\text{K}$  sources (independent variables). It must be noted that the results of Monte Carlo calculation are normalized to one source gamma. By performing this fitting procedure for each sample, three scale factors ( $f_i$ ) were achieved which represent the contribution of  $^{238}\text{U}$ ,  $^{232}\text{Th}$ , and  $^{40}\text{K}$ , in creating of the measured spectrum. The activity concentration for each radioactive isotope can be obtained by the following equation

$$A_i^j = \frac{f_i^j}{N_{\gamma/d}^j m_j} \quad (1)$$

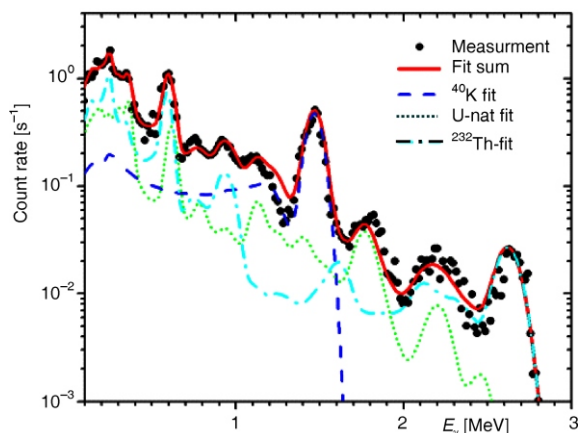


**Figure 1.** A typical measured pulse-height spectrum in MCA with the results of full-spectrum fitting procedure

where  $j$  is the granite sample-identifying index,  $N_{\gamma/d}^j$  – the average number of gammas emitted per disintegration of the parent and given in tab. 1, and  $m_j$  – the sample mass in kg.

Figure 1 shows a measured gamma spectrum of a sample (solid points) with the results of full-spectrum fitting procedure. The simulated spectra are shown with different line styles:  $^{238}\text{U}$  (short dot),  $^{232}\text{Th}$  (dash dotted), and  $^{40}\text{K}$  (dashed). The sum of the simulated spectra is shown as the solid line.

In the following section, we focus on interpreting the results obtained from various samples. The results of the activity concentrations of  $^{238}\text{U}$ ,  $^{232}\text{Th}$ , and  $^{40}\text{K}$  in different samples are shown in tab. 2. The specified activity

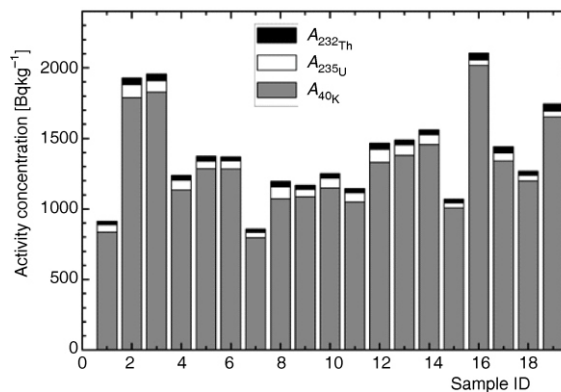


**Figure 2.** Activity concentrations of 19 decorative granite samples of Iran: white for  $^{238}\text{U}$ , black for Th series and gray columns for  $^{40}\text{K}$  in  $\text{Bqkg}^{-1}$

of  $^{40}\text{K}$  is higher with respect to the case of  $^{238}\text{U}$  and  $^{232}\text{Th}$  (in tab. 2). The activity concentrations of  $^{238}\text{U}$ ,  $^{232}\text{Th}$ , and  $^{40}\text{K}$  ranged from 32.3 to 92.6  $\text{Bqkg}^{-1}$ , 23.9 to 52.2  $\text{Bqkg}^{-1}$ , and 796.5 to 2018.4  $\text{Bqkg}^{-1}$ , respectively. The average values of 60.5  $\text{Bqkg}^{-1}$ , 36.6  $\text{Bqkg}^{-1}$ , and 1299.4  $\text{Bqkg}^{-1}$  were also obtained for  $^{238}\text{U}$ ,  $^{232}\text{Th}$ , and  $^{40}\text{K}$ , respectively. Figure 2 shows these concentrations for individual radionuclides in columns.

**Table 2.** Concentrations of  $^{238}\text{U}$ ,  $^{232}\text{Th}$ , and  $^{40}\text{K}$  in the different decorative granite samples of Iran

Sample region	Sample ID	$A_{\text{U}}$ [ $\text{Bqkg}^{-1}$ ]	$A_{\text{Th}}$ [ $\text{Bqkg}^{-1}$ ]	$A_{\text{K}}$ [ $\text{Bqkg}^{-1}$ ]
Urmia-Takab	1	50.5	23.9	836.9
Zanjan-Blue	2	92.6	46.9	1788.1
Zanjan-Beige	3	81.2	45.9	1828.3
Qazvin	4	68.7	34.6	1134.3
Hamedan-Black	5	52.5	35.6	1285.6
Borujerd	6	55.3	30.2	1283.4
Isfahan-Red	7	36.4	25.7	796.5
Isfahan-Natanz	8	83.9	41.5	1071.4
Isfahan-Naein	9	52.4	30.8	1086.7
Yazd-Diamond	10	70.2	33.3	1147.5
Yazd-Red	11	64.8	29.5	1048.5
Yazd-Rabbit	12	91.5	46.6	1329.8
Nehbandan-White	13	75.2	34.3	1378.8
Nehbandan-Orange	14	68.9	35.3	1456.4
Nehbandan-Black	15	32.3	27.7	1008.4
Zahedan-Orange	16	37.3	47.9	2018.4
Zahedan	17	58.8	44.6	1338.8
Zahedan-Kh	18	38.3	29.3	1199.1
Taibad	19	39.5	52.2	1652.4
Average		60.5	36.6	1299.4

### Radiological doses and hazard indices

The main concern of using the granite stones in the building materials is the radiation dangers to humans due to the gamma-ray emissions of radionuclides inside them. Therefore, measuring the radiological hazard indices is very important to manage these materials. In the following, some of our calculations regarding radiation doses and hazard indices are discussed.

#### Radium equivalent activity ( $Ra_{eq}$ )

The essential contribution of the natural radioactivity comes from the gamma-ray emitted by materials which contain  $^{238}\text{U}$ ,  $^{232}\text{Th}$ , and  $^{40}\text{K}$ . The radioecology of these substances is defined as Equivalent Radium Activity ( $Ra_{eq}$ ) in terms of  $\text{Bqkg}^{-1}$ . The principal assumption of this definition is that 370  $\text{Bqkg}^{-1}$  of  $^{238}\text{U}$ , 260  $\text{Bqkg}^{-1}$  of  $^{232}\text{Th}$ , and 4810  $\text{Bqkg}^{-1}$  of  $^{40}\text{K}$  exhibit the same gamma-ray dose rate. According to the 2008 UNSCEAR report, the  $Ra_{eq}$  is defined by the following relation [14]

$$Ra_{eq} = A_{\text{U}} + 1.43A_{\text{Th}} + 0.07A_{\text{K}} \quad (2)$$

where  $A_{\text{U}}$ ,  $A_{\text{Th}}$ , and  $A_{\text{K}}$  are the activity concentrations of  $^{238}\text{U}$ ,  $^{232}\text{Th}$ , and  $^{40}\text{K}$  families in  $\text{Bqkg}^{-1}$ , respectively, shown in tab. 2. Table 3 shows the  $Ra_{eq}$  for 19 samples of granite ranged from 134.5  $\text{Bqkg}^{-1}$  to 297.6  $\text{Bqkg}^{-1}$  with the average value of 212.9  $\text{Bqkg}^{-1}$  which is lower than the maximum value reported by UNSCEAR [19] and

**Table 3. The  $Ra_{eq}$  [Bqkg<sup>-1</sup>], absorbed dose rate  $D$  [nGyh<sup>-1</sup>], annual effective dose rate (AEDR;  $\mu$ Svy<sup>-1</sup>) and external and internal hazard indices for granite samples of Iran**

Sample ID	$Ra_{eq}$ [Bqkg <sup>-1</sup> ]	$D$ [nGyh <sup>-1</sup> ]	AEDR [ $\mu$ Svy <sup>-1</sup> ]	$H_{ex}$	$H_{in}$
1	149.1	72.7	89.1	0.4	0.5
2	297.6	145.7	178.7	0.8	1.1
3	287.6	141.5	173.5	0.8	0.9
4	205.5	99.9	122.6	0.5	0.7
5	202.4	99.4	121.9	0.5	0.7
6	197.2	97.3	119.3	0.5	0.7
7	134.5	65.6	80.4	0.4	0.5
8	225.8	108.5	133.1	0.6	0.8
9	180.1	88.1	108.1	0.5	0.6
10	206.2	100.4	123.1	0.6	0.7
11	187.7	91.5	112.2	0.5	0.7
12	260.5	125.9	154.4	0.7	0.9
13	230.4	112.9	138.5	0.6	0.8
14	231.5	113.9	139.7	0.6	0.8
15	149.6	73.7	90.4	0.4	0.5
16	261.2	130.3	159.8	0.7	0.8
17	225.7	109.9	134.8	0.6	0.8
18	172.6	85.4	104.8	0.5	0.6
19	241.4	118.7	145.6	0.6	0.8
Average	212.9	104.3	127.9	0.6	0.7

NEA-OECD [20] (the recommended values are less than 370 Bqkg<sup>-1</sup>). The radium equivalent activities calculated for rocks in some areas in the world are as follows: 9-239 Bqkg<sup>-1</sup> in Malaysia [10], 29-72 Bqkg<sup>-1</sup> in Egypt [8], the average value of 498 Bqkg<sup>-1</sup> in Turkey [21], and 39-122 Bqkg<sup>-1</sup> in Saudi Arabia [22].

*Gamma radiation dose rate (D)*

The absorbed dose rate is the energy deposited in a medium by ionizing radiation per unit of time. The absorbed dose rate in air 1 meter above the ground level is [14]

$$D[nGyh^{-1}] = 0.462A_U + 0.604A_{Th} + 0.417A_K \quad (3)$$

Table 3 shows the measured absorbed dose rate for all samples, ranging from 65.6 nGyh<sup>-1</sup> to 145.7 nGyh<sup>-1</sup>, with the mean value of 104.3 nGyh<sup>-1</sup> which was greater than the population-weighted value reported by NSCEAR 2008 (59 nGyh<sup>-1</sup>). The dose rates reported in the various references have been 4-112 nGyh<sup>-1</sup> in Malaysia [10], 5-45 nGyh<sup>-1</sup> in Egypt [8], 219 nGyh<sup>-1</sup> in Turkey [21], and 18-54 nGyh<sup>-1</sup> in Saudi Arabia [22].

*Annual effective dose rate (AEDR)*

The annual effective dose rate is proportional to the absorbed dose rate in air with two coefficients: 0.7 Sv/Gy conversion coefficient from the absorbed dose rate in air to effective dose equivalent received by adult and 0.2 occupancy fraction for the outdoor. The annual effective dose rate (AEDR) is given by

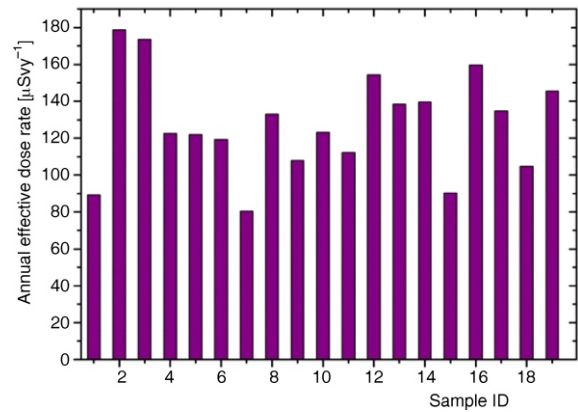


**Figure 3. The annual effective dose rates for granite samples investigated in this work**

$$AEDR (\mu Svy^{-1}) = D [nGyh^{-1}] \times 8760 [hy^{-1}] \times 0.2 \times 0.7 \times 10^{-3} \quad (4)$$

The values of the annual effective dose rate for the granite samples are presented in tab. 3. Figure 3 also depicts these values ranging from 80.4  $\mu$ Svy<sup>-1</sup> to 178.7  $\mu$ Svy<sup>-1</sup> with the mean value of 127.9  $\mu$ Svy<sup>-1</sup>. These mean values were also compared with those reported by the UNSCEAR 2008, *i. e.*, 70  $\mu$ Svy<sup>-1</sup> [19], Malaysia, *i. e.*, 72  $\mu$ Svy<sup>-1</sup> [10], and Turkey, *i. e.*, 269  $\mu$ Svy<sup>-1</sup> [21].

*External and internal hazard indices ( $H_{ex}$ ,  $H_{in}$ )*

The values of the external and internal hazard indices must be less than unity to neglect the radiation hazard. The  $H_{ex}$  and  $H_{in}$  hazard indices were calculated from the following formula

$$H_{ex} = \frac{A_U}{370} + \frac{A_{Th}}{259} + \frac{A_K}{4810} \quad (5)$$

$$H_{in} = \frac{A_U}{185} + \frac{A_{Th}}{259} + \frac{A_K}{4810} \quad (6)$$

Table 3 shows the values of  $H_{ex}$  and  $H_{in}$  for various samples, ranging from 0.4 (0.5) to 0.8 (1.1) with average of 0.6 (0.7); fig. 4 indicates the  $H_{ex}$  and  $H_{in}$  for

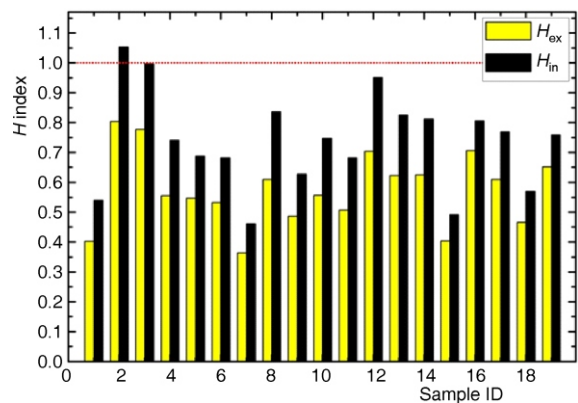


**Figure 4. The external and internal hazard indices for granite samples investigated in this work. The dotted red line depicts the maximum value allowed for the  $H_{in}$**

all samples. In the second sample (sample ID = 2), the  $H_{in}$  was higher than unity. Therefore, using this sample in the building material is not advised.

## CONCLUSION

The natural radioactivity due to the presence of  $^{238}\text{U}$ ,  $^{232}\text{Th}$ , and  $^{40}\text{K}$  in the decorative granite stones in some parts of Iran was evaluated using the gamma-ray spectroscopy. The results showed that the radium equivalent activity and the external and internal hazard indices were lower than the worldwide average and the gamma radiation dose rate and annual effective dose rate were greater than the average value. The results in fig. 4 show that the samples No. 2, 3, 16, and 19 have the highest concentration of radionuclides. The higher concentrations of radionuclides in some samples depended on the geological features of the areas where the granites belong. These samples belonged to Zanjan, Khorasan, and Zahedan Provinces of Iran. The hazard indices showed that only the second sample had the  $H_{in}$  higher than unity. Therefore, in most of the samples investigated in this study, the radiological hazard was below the recommended values.

## AUTHORS' CONTRIBUTIONS

Preparation of the samples was done by M. Hassanvand. Measurements and computational work was carried out by R. Khabaz. The analysis on results was carried out by M. Hassanvand. The manuscript was written and reviewed by both authors.

## ACKNOWLEDGEMENT

This work was supported by the Golestan University, Iran, under contract of Research Project No. 961528.

## REFERENCES

- [1] Arafa, W., Specific Activity and Hazard of Granite Samples Collected from the Eastern Desert of Egypt, *Journal of Environmental Radioactivity*, 75 (2014), 3, pp. 315-327
- [2] Larsen, S., Gottfried, D., Uranium and Thorium in Selected Suites of Igneous Rocks, *American Journal of Science*, 258 (1960), A, pp.151-169
- [3] Llope, W. J., Activity Concentrations and Dose Rates from Decorative Granite Countertop, *Journal of Environmental Radioactivity*, 102 (2011), 6, pp. 620-629
- [4] Uosif, M. A. M., Quantitative Measurement of Natural Radioactivity in Some Roofing Tile Materials Used in Upper Egypt, *Radiation Protection Dosimetry*, 156 (2013), 2, pp. 231-238
- [5] Nikolić, M. D., Simović, R. D., Radon Exhalation Rates of Some Granites Used in Serbia, *Nucl Technol Radiat*, 30 (2015), 2, pp. 145-148
- [6] Khabaz, R., Estimation of Scattering Contribution in the Calibration of Neutron Devices with Radionuclide Sources in Rooms of Different Sizes, *Nucl Technol Radiat*, 30 (2015), 1, pp. 47-54
- [7] El-Taher, A., Gamma Spectroscopic Analysis and Associated Radiation Hazards of Building Materials Used in Egypt, *Radiation Protection Dosimetry*, 138 (2010), 2, pp. 166-173
- [8] El-Taher, A., et al., Natural Radioactivity Levels and Radiation Hazard Indices in Granite from Aswan to Wadi El-Allaqi Southeastern Desert, Egypt, *Radiation Protection Dosimetry*, 124 (2007), 2, pp.148-154
- [9] Yang, Y.-X., et al., Radioactivity Concentrations in Soils of the Xiazhuang Granite Area, China, *Applied Radiation and Isotopes*, 63 (2005), 2, pp. 255-259
- [10] Alnour, I. A., et al., Assessment of Natural Radioactivity Levels in Rocks and their Relationship with the Geological Structure of Johor State, Malaysia, *Radiation Protection Dosimetry*, 158 (2014), 2, pp. 201-207
- [11] Bavarnequina, E., et al., Radon Exhalation Rate and Natural Radionuclide Content in Building Materials of High Background Areas of Ramsar, *Journal of Environmental Radioactivity*, 117 (2013), 1, pp. 36-40
- [12] Nassiri, P., et al., Evaluation of Radon Exhalation Rate from Granite Stone, *Journal of Scientific and Industrial Research*, 70 (2011), 3, pp. 230-231
- [13] Asgharizadeh, F., et al., Natural Radioactivity in Granite Stones Used as Building Materials in Iran, *Radiation Protection Dosimetry*, 149 (2012), 3, pp. 321-326
- [14] Hendriks, P. H. G. M., Full-Spectrum Analysis of Natural  $\gamma$ -Ray Spectra, *Journal of Environmental Radioactivity*, 53 (2001), 3, pp. 365-380
- [15] \*\*\*, MCNPX-A General Monte-Carlo N-Particle Transport Code: Version 2.6, LANL Report, LA-CP-07-1473, Los Alamos, (Ed. D. B. Pelowitz), N. Mex., USA, 2008
- [16] \*\*\*, McConn, et al., Compendium of Material Composition Data for Radiation Transport Modeling, PNNL-15870, Rev. 1, Pacific Northwest National Laboratory, Richland, Washington, 2011
- [17] \*\*\*, Evans, M. L., Calculation of Terrestrial Gamma-Ray Fields in Airborne Radiometric Surveys. Los Alamos National Laboratory, LS-9471-MS, N. Mex., USA, 1983
- [18] Khabaz, R., Yaghobi, F., Design and Employment of a Non-Intrusive  $\gamma$ -Ray Densitometer for Salt Solutions, *Radiation Physics and Chemistry*, 108 (2015), 1, pp. 18-23
- [19] \*\*\*, UNSCEAR, Sources and Effects of Ionizing Radiation: Report to the General Assembly, with Scientific Annexes, vol 1, United Nations, New York, (2010), pp. 1-219
- [20] \*\*\*, NEA-OECD, Nuclear Energy Agency: Exposure to Radiation from Natural Radioactivity in Building Materials, Report by NEA Group of Experts, OECD, Paris, 1979
- [21] Merdanoglu, B., Altinsoy, N., Radioactivity Concentrations and Dose Assessment for Soil Samples from Kestanbol Granite Area, Turkey, *Radiation Protection Dosimetry*, 121 (2006), 4, pp. 399-405
- [22] El-Taher, A., Assessment of Natural Radioactivity Levels and Radiation Hazards for Building Materials Used in Qassim Area, Saudi Arabia, *Romanian Journal of Physics*, 57 (2012), 3, pp. 726-735

Received on May 27, 2017

Accepted on August 16, 2017

**Рахим КАБАЗ, Марјам ХАСАНВАНД**

**КОНЦЕНТРАЦИЈА РАДИОАКТИВНОСТИ И ДОЗНЕ  
КАРАКТЕРИСТИКЕ ГРАНИТА**

Користећи NaI(Tl) сцинтилациони детектор (10.6 cm × 10.16 cm) високе ефикасности, одредили смо концентрације радионуклида  $^{238}\text{U}$ ,  $^{232}\text{Th}$  и  $^{40}\text{K}$  у различитим узорцима гранитног камења. Активности  $^{238}\text{U}$ ,  $^{232}\text{Th}$  и  $^{40}\text{K}$  одређене су и забележене анализом укупног спектра, а концентрације радионуклида за  $^{238}\text{U}$ ,  $^{232}\text{Th}$  и  $^{40}\text{K}$  износиле су  $32.3\text{--}92.6 \text{ Bqkg}^{-1}$ ,  $23.9\text{--}52.2 \text{ Bqkg}^{-1}$  и  $796.5\text{--}2018.4 \text{ Bqkg}^{-1}$ , респективно. Прорачун јачине доза и индекса радијационог ризика такође је обухваћен овом анализом.

*Кључне речи: сиекћиромејрија гама зрачења, NaI(Tl), радиоактивносћ, дозна каракћеристћика, гранит, MCNPX*

---